Journal of Food Engineering 229 (2018) 65–71

Contents lists available at ScienceDirect

Journal of Food Engineering

journal homepage: www.elsevier.com/locate/jfoodeng

High hydrostatic pressure induced changes on palm stearin emulsions

Sezen Sevdin [a, b], Baris Ozel [b, c], Umut Yucel [d], Mecit Halil Oztop [b], Hami Alpas [b, *]

[a] Istanbul Kultur University, Nutrition and Dietetics Department, 34191, Istanbul, Turkey
[b] Middle East Technical University, Food Engineering Department, 06800, Ankara, Turkey
[c] Ahi Evran University, Food Engineering Department, Kirsehir, Turkey
[d] Kansas State University, Food Science Institute, Mid-Campus Drive North, Manhattan, KS, USA

ARTICLE INFO

Article history:
Received 25 January 2017
Received in revised form
11 August 2017
Accepted 11 October 2017
Available online 25 October 2017

Keywords:
High hydrostatic pressure
Lipid crystallization
Transverse relaxation time
Self-diffusion coefficient
Storage time

ABSTRACT

Emulsions are thermodynamically unstable systems formed through blending of two immiscible fluids. Recent studies have shown that High Hydrostatic Pressure (HHP) can initiate or accelerate lipid crystallization in emulsions. In this study, the effect of HHP on lipid crystallization was examined. Emulsion samples were prepared with palm stearin (PS) as the oil phase and sodium caseinate (SC) as the emulsifier and they were pressurized at 100 and 500 MPa at 10, 20 and 40 °C for 15 min. In order to determine the crystal structure of the emulsions, differential scanning calorimeter (DSC) was used and the change in the crystal morphology during 28 day-storage at 4 °C was observed. Nuclear Magnetic Resonance Relaxometry (NMR) experiments were also conducted and transverse relaxation time (T_2) and self-diffusion coefficient (SDC) values showed a trend to follow polymorphic changes of lipid crystals. Results showed that pressure and storage time both had significant effects ($p < 0.05$) on the crystal structures of emulsions.

1. Introduction

Emulsions make significant contribution to control physical properties, flavors and stability in food systems (Whittinghill et al., 2000). They are thermodynamically unstable systems which contain two immiscible liquids, generally oil and water, and one liquid disperses as small droplets (dispersed phase) in the other liquid (continuous phase). Emulsions have different destabilization mechanisms but the most common ones are creaming, flocculation and coalescence (Palanuwech and Coupland, 2003; McClements, 2005; Tadros, 2013). Creaming is caused by density differences between continuous and dispersed phases and denser layer is formed at the bottom of the emulsions. Therefore, it may increase the rate of other destabilization mechanisms' occurrence (Tadros, 2013). Flocculation is a process in which droplets come together and form a three-dimensional structure but in this structure, droplets maintain their integrity. Flocculation also causes significant changes in emulsions' physicochemical and sensorial properties like texture, viscosity, shelf life and appearance (McClements, 2005). Coalescence is similar with flocculation regarding droplet gathering but in this mechanism droplets merge with each other and do not maintain their integrity. Coalescence also causes an increase in the creaming rate due to bigger sizes of droplets (McClements, 2005; Ritzoulis, 2013).

Some emulsions may have more complex structures because they contain totally or partially crystallized phases (dispersed and/or continuous phases) (Palanuwech and Coupland, 2003). In oil-in-water emulsion, fat crystals in oil droplets may initiate destabilization mechanisms via partial coalescence. Fat crystals in a droplet can interfere with crystals of another droplet and make a link between these two droplets. However, each droplet can preserve their integrity through their internal crystal structures' mechanical strength. When an emulsion is heated, fat crystals melt, droplets' integrity are lost and they finally merge with each other which triggers the coalescence (Boode and Walstra, 1993; Dickinson and McClements, 1995; Vanapalli et al., 2002; Palanuwech and Coupland, 2003; McClements, 2005). Partial coalescence rate depends on particle size and volume fraction of dispersed phase, emulsifier type and concentration, solid fat content and crystal structure (Dickinson and McClements, 1995; Palanuwech and Coupland, 2003; McClements, 2005).

Lipid crystallization consists of three steps namely; supercooling, nucleation and crystal growth. Oil can preserve its liquid phase for sometime below its crystallization temperature. The time

* Corresponding author.
E-mail address: imah@metu.edu.tr (H. Alpas).

https://doi.org/10.1016/j.jfoodeng.2017.10.007
0260-8774/

span until the first crystal nuclei can be observed is named as supercooling. Nucleation is the step where crystal nuclei are formed all over the system (Coupland, 2002). After nucleation, crystals start to grow around each nuclei and this step is called crystal growth. However, lipids can form different crystal structures that are called polymorphs. Polymorphs are generally classified in three forms, α, β′ and β-crystals but some fats have more polymorphic structures. Lipids first crystallize into α and β' forms (which are less stable), and then turn to denser β-crystals (Coupland, 2002; Zulkurnain et al., 2016a). Initial crystal structure and the rate of polymorphic change may be affected by internal (triglyceride content, structure, molecular interactions, etc.) and external (temperature-time applications, mechanical mixing, etc.) factors (McClements, 2005).

Palm stearin (PS) is the highly saturated solid part of palm oil and produced by fractionation process. PS contains different types of triacylglycerol with different ratios so melting temperatures of PS can vary. The polymorphism of PS cannot be fully understood due to this different composition (Sonoda et al., 2004).

Sodium caseinate (SC) is a protein obtained from casein, a milk protein, by means of acid-coagulation with sodium hydroxide. It is an amphiphilic molecule and provides a strong stability against steric and electrostatic repulsions between emulsion droplets. SC is used in food industry in a wide range of products as emulsifier because of its emulsification, water-binding, fat-binding, thickening, gelation and whipping properties.

Nuclear Magnetic Resonance (NMR) relaxometry is used as a non-destructive method to analyze the interior composition of complex food systems (Greiff et al., 2014). It may provide characterization of such systems via proton relaxation experiments by measuring transverse relaxation time (T_2) (also known as spin-spin relaxation time). T_2 measurement is a good tool not only to reveal the internal compositions of foods, in this case emulsions, since each organic material possesses a distinct relaxation time characteristic (Barrabino et al., 2014; Zhang et al., 2016), but also to characterize the degree of water-surrounding network interactions within a system. Self-diffusion coefficient (SDC) -characterizing the mobility of water molecules within food materials-is also measured to support the T_2 results (Salami et al., 2013).

In literature, there are some studies investigating the effects of HHP on crystal polymorphism by NMR measurements but they mainly focus on NMR spectroscopy experiments, free induction decay (FID) of sole crystals and transverse relaxation of sole crystal components (Bouteille et al., 2013; Mazzanti et al., 2008; Nadakatti, 1999; Van Duynhoven et al., 2002). To the best of our knowledge the effect of HHP on lipid crystallization in emulsions is quite a new area of interest and has not been explored extensively despite limited number of studies with conflicting observations in the literature. Oh and Swanson (2006), claimed that crystallization rate of cocoa oil emulsions was not affected ($p > 0.05$) and only their polymorphic structure could be slightly changed by the HHP treatment up to 600 MPa. On the other hand, Blümer and Mäder (2005) and Ferstl et al. (2011) reported that HHP treatment (at 200–750 MPa and 4–48 °C for 5–30 min) could be used to modulate the microstructure of crystalline lipid droplets. High pressure values (300–600 MPa) caused substantial reduction in lipid volume (17–30%) (Rostocki et al., 2013) due to weak Van der Waals interactions that were easily overcame by pressure treatments (Zulkurnain et al., 2016b). HHP is more effective on saturated fatty acids than unsaturated ones, consequently leading to faster crystallization of saturated fatty acids. Application of HHP decreases the specific surface energy needed for crystallization thus, induces crystal nucleation in an energy efficient way and affects the polymorphism of such crystals (Zulkurnain et al., 2016b).

The objective of this study is to i) observe and track the effect of HHP treatment on the crystal structure of an emulsion produced with PS as disperse phase and SC as emulsifier, by NMR relaxometry method, ii) provide transverse relaxation profile for the whole emulsion system and iii) supply information on the overall crystallization process and mechanisms taking place within the emulsion system. NMR relaxometry was proposed as an alternative method to understand polymorphic changes of lipid crystals due to HHP treatment and during storage period.

2. Materials and methods

2.1. Materials

Palm stearin (PS) (fully hydrogenated palm stearin with a min 55 °C melting point) was donated by Cargill Turkey (Bursa, Turkey). Casein sodium salt (C8654) was purchased from Sigma-Aldrich (St. Louis, Missouri, USA).

2.2. Emulsion preparation

Hot homogenization technique was used for emulsion preparation (Yucel et al., 2013). Sodium caseinate solution (2 wt %) was prepared with double distilled water, stirred overnight and heated up to 80 °C for 1 h. Palm stearin was incubated at 70 °C for 30 min to ensure that all crystal structures were melt. Palm stearin and sodium caseinate solution were mixed with a ratio of 1:9 (w/w) by using T18 digital ULTRA TURRAX® (IKA, Staufen, Germany) with a speed of 1000 rpm for 30 s. This coarse emulsion was passed 3 times through M-110Y Microfluidizer® (Microfluidics Corporation, MA, USA) at 100 MPa at 60-65 °C. The hot samples were stored at 45 °C (i.e., above crystallization temperature of PS droplets) for less than 1 h in water bath until HHP treatment.

2.3. High hydrostatic pressure (HHP) treatment

HHP applications were performed with type-760.0118 high hydrostatic equipment (SITEC, Zurich, Switzerland). The equipment consists of a pressurization chamber, two end closures, a means for restraining the end closures, a pressure pump, a hydraulic unit and a temperature control device. Pressure transmitting medium was a mixture of water and glycol. The liquid was heated prior to pressurization to the desired temperature by an electrical heating system surrounding the chamber. Pressurization chamber has 24 mm internal diameter, 153 mm length and 100 mL capacity. The rate of pressure increase and pressure release was approximately 5–10 s for the designed system. Pressurization time reported in this study did not include the pressure increase and release times.

Prepared emulsions were pressurized in 2 mL sterile cryotubes (Biosigma Srl, CLEARLINE®, CryoGen®Tubes) at two different pressure (100 and 500 MPa) and three different temperatures (10, 20 and 40 °C) for 15 min. HHP treatments were carried out at temperatures defined according to preliminary differential scanning calorimetry (DSC) experiments (Fig. 1 (Sevdin et al., 2017)) to define roughly the approximate melting and crystallization temperatures 40 °C was selected as the point where no crystal formation occur, 20 °C as the point that crystal formation depending on the temperature was completed and 10 °C as a low reference temperature. Pressure levels were selected to be one low and one high level as 100 and 500 MPa. Pressure application time was constant and relatively longer than general HHP applications to remove the effect of time on the crystal formation. At the end of the processing time, samples were held at room temperature until the analyses were completed. They were then stored at refrigeration temperature (4 °C) for 28 days.

Following HHP application, abbreviations were implemented

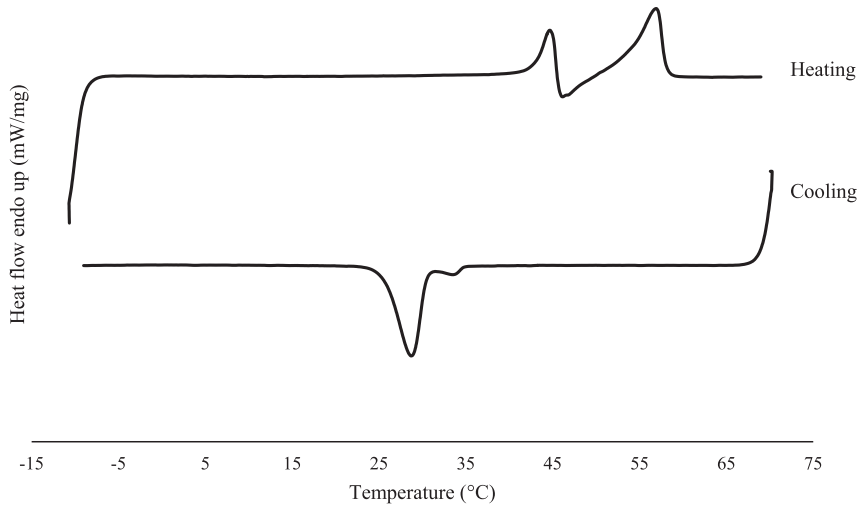

Fig. 1. Differential Scanning Calorimetry (DSC) heating and cooling thermograms of unpressurized palm stearin-sodium caseinate sample at first day (heat flow was normalized to sample weight).

for naming HHP treated samples and defining the treatment conditions. If a sample was pressurized at 500 MPa at 10 °C for 15 min it was named as 500_10_15 and "unpressurized" is used for the untreated control sample.

2.4. Differential scanning calorimetry (DSC) analysis

DSC 4000 (Perkin Elmer, MA, USA) was used to determine the crystallization and melting temperatures of polymorphs. 10 mg sample was placed into a DSC pan and the pan was hermetically sealed. An empty aluminum DSC pan was used as reference. Purge gas was N_2 with a flow rate of 19.8 mL/min. DSC was calibrated with zinc provided by the producer (Perkin Elmer) (99.995% purity) according to the operator's manual. Applied thermal cycle was as follows: heating from 35 to 70 °C with a rate of 2.5 °C/min, holding for 5 min at 70 °C and cooling from 70 to −10 °C at a rate of 2.5 °C/min. All samples were subjected to DSC analysis at the 1st, 8th, 14th and 28th days of storage. To calculate the relative content of polymorphs in a sample (expressed as %), the area under each peak was determined and divided by the total area of all peaks. However, during melting process, at the end of the 1st peak, an exothermic reaction was observed due to re-crystallization. Re-crystallization during melting cycle was also observed in pure palm stearin DSC thermograph (Supplement A). Since this exothermic reaction was observed in all emulsion samples, a baseline was used to calculate the area under 1st peak by omitting the re-crystallization part. The baseline for each sample was set as a line between the starting point of 1st peak and the end point of last peak. The area between the peak and the baseline was used to determine the percent polymorph content by omitting the re-crystallization part.

2.5. Nuclear magnetic resonance (NMR) relaxometry measurements

Spin-spin relaxation time experiments (T_2) were conducted on a 0.5 T NMR spectrometer operating at a Larmor frequency of 23.2 MHz, equipped with a 10-mm diameter radio frequency coil (SpinCore Inc., Gainsville, FL, USA). Carr-Purcell-Meiboom-Gill (CPMG) pulse sequence was used to record relaxation data with 1 ms echo time, 2000 echoes, 16 scans and 3s repetition time. For self-diffusion coefficient (SDC) measurements, stimulated spin echo pulse sequence containing three 22 us, 90° was used in a 0.32 T NMR system (Spin Track SB4, Mary El, Russia). The time intervals between the first and the second pulses and between the second and the third pulses were 2 ms and 60 ms, respectively. Acquisition time was 500 us. The duration of the pulsed gradient field was 1 ms and the gradient strength was 1.66e-2 T/m.

2.6. Statistical analysis

Experiments were conducted in triplicate. Minitab 17 was used to analyze the results (Minitab Inc., Penn State, USA). ANOVA was conducted at 95% confidence interval. Tukey multiple comparison test was applied to differentiate the similarity between the samples.

3. Results and discussion

DSC was used to determine the melting and crystallization temperature of polymorphs and their percent ratios in the emulsion. DSC analysis limits were determined according to preliminary experiments which showed the melting temperature of PS emulsions occurring between 40 and 57 °C and crystallization occurring between 35 and 23 °C (data not shown). Accordingly, the heating step was set up from 35 to 70 °C to characterize the crystalline structure and polymorphic form and the cooling step from 70 to −10 °C to observe the onset point of crystallization and differentiate surface crystallization properties. Heating and cooling thermograms of samples which were pressurized at 500 MPa at 20 °C and 40 °C are reported in Fig. 2 as representative thermograms (all thermograms were not shown).

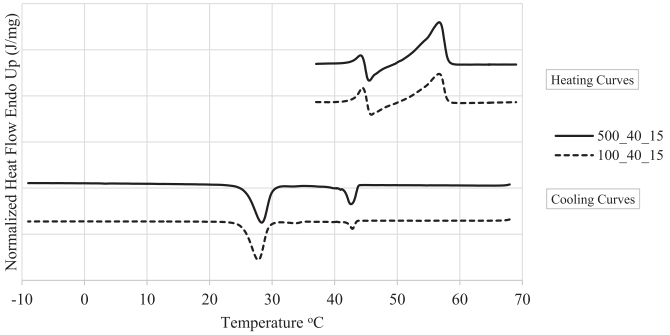

Fig. 2. DSC thermograms of selected samples. Top lines show the heating step and bottom lines show the cooling step.

The melting thermograms contained two peaks which indicated that there were two different crystal structures in emulsions. The first peak which has a melting temperature around 45 °C, corresponded to α-crystal structure and the second one which has a melting temperature around 56 °C, to β-crystal structures (Sonoda et al., 2004). The area of these peaks in melting thermograms were used to calculate the crystal content in emulsions (Table 1). In the cooling thermograms, two peaks at around 28 and 43 °C were seen, showing that system crystallized with two polymorphic structure: α and β crystals (Sonoda et al., 2004). From the thermograms obtained, it can be concluded that HHP treatment within the conditions of the study did not change the melting and crystallization temperatures of the solid lipid crystals in emulsion droplets ($p > 0.05$), (data was not shown), but it has the ability to change the polymorphic structure in emulsions significantly ($p < 0.05$) (Table 1). At the end of 1st day, all pressurized samples contained lower α-crystal and higher β-crystal than the unpressurized samples (Table 1). The samples pressurized at 500 MPa at 10 °C (500_10_15) and 20 °C (500_20_15) had the lowest α -crystal content. α-crystal content of samples changed significantly within 1 week of storage ($p < 0.05$) and did not show any further significant change during the storage period (except 500_10_15 sample). It is claimed that HHP (at 600 MPa, 90 °C for 10 min) enforces the system to reduce in volume so crystal structures align themselves in more dense forms, in this case β form (Zulkurnain et al., 2016a).

HHP caused an increase in the degree of molecular ordering and packing leading to formation of a more stable network as it provided higher percentage of β forms in the emulsion at 500 MPa compared to unpressurized samples as shown in Table 1 ($p < 0.05$). This trend was also proved by NMR relaxometry measurements. The steep increase in β form and decrease in α form (transformation of α crystals to β crystals) after 500 MPa, resulted in a significant increase in T_2 values of emulsions especially after 28 day of storage time ($p < 0.05$) (Fig. 3). Formation of β crystals was associated with a close and compact alignment of crystallized lipid molecules but the increase in T_2 values also suggested that the overall emulsion system experienced a higher proton relaxation time. The reasons behind the higher proton relaxation times were proposed as i) expelling of water from the surroundings of crystal lattices due to the close conformation of such crystals after HHP and ii) expelling of encapsulated materials in emulsions from highly ordered lipid crystals since the incorporation of such encapsulated materials into the crystals were hardly possible (Blümer and Mäder, 2005). Therefore, the relocation of water and encapsulated materials in the polar environment of the continuous liquid-like phase contributed to the higher T_2 values. The close and compact alignment of lipid crystals slightly increased the sample density which in turn increased the spatial density of protons within the sensing volume of the radio frequency coil and resulted in an overall higher signal (Mazzanti et al., 2008). Additionally, the decreased interaction

Table 1
α- and β-crystal content (%) of samples. Capital letters show a sample's significant difference between its α- and β-crystal contents with respect to storage time. Small letters show samples' α- and β-crystal content differences at a specific day meaning the differences in each column. α- and β-crystal contents are compared in themselves. The results that do not share a letter are significantly different with 95% confidence interval ($p < 0.05$). Errors are represented as standard deviations between replicates.

Samples	1st day		8th day		14th day		28th day	
	α content (%)	β content (%)	α content (%)	β content (%)	α content (%)	β content (%)	α content (%)	β content (%)
unpressurized	$57.69 \pm 1.43^{A,a}$	$42.31 \pm 1.43^{B,d}$	$17.39 \pm 4.93^{B,ab}$	$82.34 \pm 4.93^{A,b}$	$12.29 \pm 3.24^{B,b}$	$87.71 \pm 3.24^{A,b}$	$13.70 \pm 4.64^{B,a}$	$86.30 \pm 4.64^{A,a}$
100_10_15	$25.77 \pm 4.17^{A,cd}$	$74.07 \pm 4.17^{B,ab}$	$13.16 \pm 1.34^{B,abc}$	$86.84 \pm 1.34^{A,ab}$	$8.2 \pm 1.36^{B,bc}$	$91.80 \pm 1.36^{A,ab}$	$11.83 \pm 3.86^{B,a}$	$88.17 \pm 3.86^{A,a}$
100_20_15	$34.84 \pm 5.47^{A,c}$	$65.01 \pm 5.47^{B,b}$	$19.47 \pm 1.85^{B,a}$	$80.53 \pm 1.85^{A,b}$	$9.49 \pm 1.45^{B,bc}$	$90.51 \pm 1.45^{A,ab}$	$16.65 \pm 4.82^{B,a}$	$83.19 \pm 4.82^{A,a}$
100_40_15	$47.02 \pm 3.34^{A,ab}$	$52.98 \pm 3.34^{B,cd}$	$12.05 \pm 0.19^{B,abc}$	$87.95 \pm 0.19^{A,ab}$	$17.79 \pm 1.45^{B,a}$	$82.21 \pm 1.45^{A,c}$	$18.13 \pm 1.75^{B,a}$	$81.87 \pm 1.75^{A,a}$
500_10_15	$16.47 \pm 0.78^{A,d}$	$83.53 \pm 0.78^{C,a}$	$6.57 \pm 0.33^{C,c}$	$93.43 \pm 0.33^{A,a}$	$6.98 \pm 0.83^{C,bc}$	$93.02 \pm 0.83^{A,ab}$	$10.25 \pm 0.92^{B,a}$	$89.54 \pm 0.92^{B,a}$
500_20_15	$18.27 \pm 1.05^{A,d}$	$81.73 \pm 1.05^{B,a}$	$8.49 \pm 3.07^{B,bc}$	$91.51 \pm 3.07^{A,ab}$	$8.13 \pm 0.08^{B,bc}$	$91.87 \pm 0.08^{A,ab}$	$7.02 \pm 1.82^{B,a}$	$92.98 \pm 1.82^{A,a}$
500_40_15	$34.62 \pm 3.01^{A,bc}$	$65.38 \pm 3.01^{B,bc}$	$10.50 \pm 0.36^{B,abc}$	$90.53 \pm 0.36^{A,ab}$	$6.23 \pm 0.02^{B,c}$	$93.77 \pm 0.02^{A,a}$	$9.14 \pm 1.76^{B,a}$	$90.56 \pm 1.76^{A,a}$

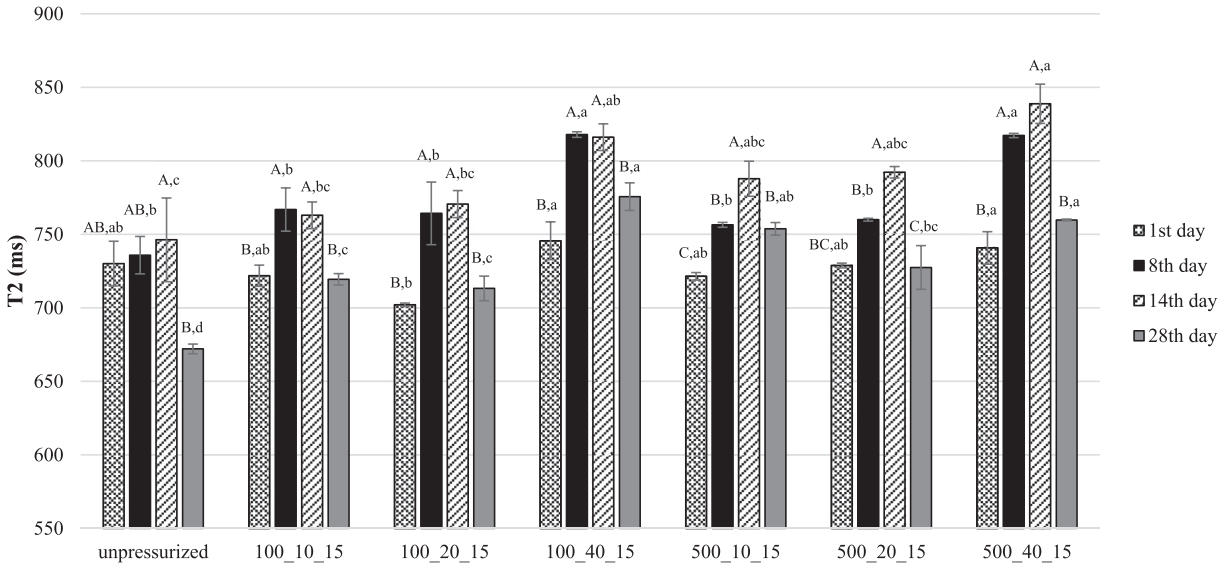

Fig. 3. T_2 of samples during storage. Capital letters show a sample's significant difference between T_2 with respect to storage time meaning that capital lettering is done for each bar group. Small letters show samples' T_2 difference for each day, for each group (1st day of 100_10_15 and 100_20_15 etc.). The results that do not share a letter are significantly different with 95% confidence interval ($p < 0.05$). The numbers above the bars are showing the storage days at which the experiments were conducted. Error bars are represented as standard deviations between replicates.

between the oil and the water phases due to the crystallization of lipid molecules could contribute to higher T_2 values since water molecules had more opportunity to interact with each other and water-water interactions took the place of the water-oil interactions eventually giving higher relaxation times.

The effects of HHP on polymorphism of lipid crystals were also evaluated by self-diffusion coefficient (SDC) measurements and results are given in Table 2. The increase in pressure and consecutive increase in β crystal formation induced lower SDC values ($p < 0.05$). Clearly, the diffusion of water molecules was hindered by pressure treatment within the emulsion. The reason could be, although in small amounts, the formation of bulk crystals in continuous phase as shown in the cooling curve. The small impurities present in the continuous phase could serve as heterogeneous nucleation sites (Vanapalli et al., 2002). The crystals formed in bulk phase might block the diffusion pathway of water molecules in certain points causing reduction in SDC of water. Moreover, the closer packing under high pressure also altered the diffusion pathway of water within the emulsion system compared to initial stage. Variation of temperature, on the other hand, did not affect the polymorphism of lipid crystals under HHP treatment denoting that the pressure and storage time parameters predominated the high-pressure crystallization process rather than temperature.

Besides the direct effects of applied pressure on α-β contents, T_2 and SDC, storage time after HHP also had significant impacts. Firstly, longer storage times induced lower α and higher β crystal contents (Table 1). The steep decrease in α content and respective increase in β content was observed between the 1st and the 8th day of storage ($p < 0.05$). The crystal ratios were more or less the same from the 8th day up to 28th day indicating that the main change in polymorphism was achieved up to 8th day of the storage.

The T_2 and SDC trends were in agreement with the changes in morphology of samples since they showed a traceable pattern with respect to changes in α and β contents. Higher T_2 on the 8th day than 1st day of storage was observed and this was in accordance with the pressure results since higher pressures thus β contents led to higher T_2 values (Fig. 3). In this way, the higher β crystal formation during storage was observed by T_2 results. 500 MPa treatment for all temperatures induced more abrupt increase in T_2 during storage proving the effect of magnitude of pressure applied on relaxation times. Reasons behind this T_2 trend was the same with pressure case such as the formation of highly ordered crystals during storage and expelling of water and encapsulated materials from surrounding crystal lattice. Despite the reverse correlation between SDC and T_2 in pressure experiments, they exerted a straight correlation in storage experiments (Table 2). Both T_2 and SDC increased up to 14th day and experienced a decrease on the 28th day ($p < 0.05$). The increase in SDC suggested that up to 14th day, water phase present in the emulsion system became more continuous.

The statistically similar particle sizes of droplets at that time interval proved the claim of continuous water phase up to 14th day, since a change in the particle size promoted discontinuity in such systems (Dickinson and Golding, 1997). Therefore, since diffusing water molecules did not experience a heterogeneous distribution of droplets in the emulsion, their SDC increased. Nevertheless, both the T_2 and SDC decreased between the 14th and 28th days. This phenomenon was also seen in overall α and β contents, with a slight increase in α crystals and slight decrease in β crystals on the 28th day with respect to 14th day. 500_10_15 samples indicated significantly higher α and lower β contents on the 28th day with respect to 14th day ($p < 0.05$). The observed changes could have been attributed to the beginning of destabilization on the 14th day of the storage since a tendency for an increase in the presence of bigger droplets throughout the emulsion was also detected by span and particle size measurements (Table 3). Span measurements showed the highest polydispersity on 14th and 28th days, this high polydispersity decreased indicating that the particle size distribution began to vary toward bigger particles on 14th day. Furthermore, the bigger particles formed on the 14th day disappeared on the 28th day since significant decrease in bigger particle size (d_{43}) and span values were observed.

Table 2
Self-diffusion coefficients (SDC) of samples during storage. Capital letters show a sample's significant difference between self-diffusion coefficients with respect to storage time. Small letters show samples' self-diffusion coefficients at a specific day meaning the differences in each column. $d_{4,3}$ and span results were compared in themselves. The results that do not share a letter are significantly different with 95% confidence interval ($p < 0.05$). Errors are represented as standard deviations between replicates.

Samples	Self-Diffusion Coefficient $*10^{-9}$ (m^2/s)			
	1st day	8th day	14th day	28th day
unpressurized	$2.2746 \pm 0.0368^{BC,a}$	$2.3617 \pm 0.0313^{B,ab}$	$2.6813 \pm 0.0135^{A,a}$	$2.1780 \pm 0.0483^{C,a}$
100_10_15	$2.1125 \pm 0.0233^{B,b}$	$2.2739 \pm 0.0091^{A,b}$	$2.3502 \pm 0.0383^{A,b}$	$2.1214 \pm 0.0612^{B,ab}$
100_20_15	$2.1531 \pm 0.0713^{B,ab}$	$2.2061 \pm 0.0268^{AB,b}$	$2.4634 \pm 0.0888^{A,ab}$	$2.1740 \pm 0.0563^{B,a}$
100_40_15	$1.9284 \pm 0.0069^{B,c}$	$2.5730 \pm 0.1640^{A,a}$	$2.4002 \pm 0.0444^{A,b}$	$1.8780 \pm 0.0211^{B,c}$
500_10_15	$2.1432 \pm 0.0295^{B,ab}$	$2.1651 \pm 0.0427^{B,b}$	$2.2861 \pm 0.0171^{A,b}$	$1.9592 \pm 0.0044^{C,bc}$
500_20_15	$2.0294 \pm 0.0331^{C,bc}$	$2.2436 \pm 0.0582^{AB,b}$	$2.3453 \pm 0.0112^{A,b}$	$2.1166 \pm 0.0659^{BC,ab}$
500_40_15	$1.9615 \pm 0.0278^{B,c}$	$2.3153 \pm 0.0214^{A,ab}$	$2.3720 \pm 0.1660^{A,b}$	$2.1668 \pm 0.0223^{AB,a}$

Table 3
Mean particle analysis and Span results of samples during storage. Capital letters show a sample's significant difference between its $d_{4,3}$ and span results with respect to storage time. Small letters show samples' $d_{4,3}$ and span results at a specific day meaning the differences in each column. $d_{4,3}$ and span results were compared in themselves. The results that do not share a letter are significantly different with 95% confidence interval ($p < 0.05$). Errors are represented as standard deviations between replicates.

Samples	1st day		8th day		14th day		28th day	
	$d_{4,3}$ (μm)	Span	$d_{4,3}$ (μm)	Span	$d_{4,3}$ (μm)	Span	$d_{4,3}$ (μm)	Span
unpressurized	$0.266 \pm 0.006^{B,a}$	$1.728 \pm 0.068^{B,a}$	$0.259 \pm 0.011^{B,a}$	$1.663 \pm 0.070^{B,a}$	$0.539 \pm 0.020^{A,ab}$	$2.413 \pm 0.162^{A,a}$	$0.276 \pm 0.002^{B,a}$	$1.701 \pm 0.001^{B,a}$
100_10_15	$0.278 \pm 0.012^{B,a}$	$1.721 \pm 0.009^{B,a}$	$0.256 \pm 0.008^{B,a}$	$1.656 \pm 0.049^{B,a}$	$0.732 \pm 0.047^{A,ab}$	$2.588 \pm 0.025^{A,a}$	$0.283 \pm 0.007^{B,a}$	$1.718 \pm 0.027^{B,a}$
100_20_15	$0.279 \pm 0.015^{A,a}$	$1.752 \pm 0.074^{B,a}$	$0.264 \pm 0.004^{A,a}$	$1.692 \pm 0.020^{B,a}$	$0.387 \pm 0.044^{A,b}$	$2.103 \pm 0.038^{A,a}$	$0.326 \pm 0.062^{A,a}$	$1.747 \pm 0.025^{B,a}$
100_40_15	$0.280 \pm 0.012^{B,a}$	$1.714 \pm 0.038^{B,a}$	$0.249 \pm 0.000^{C,a}$	$1.643 \pm 0.031^{B,a}$	$0.465 \pm 0.002^{A,ab}$	$2.221 \pm 0.034^{A,a}$	$0.287 \pm 0.004^{B,a}$	$1.729 \pm 0.010^{B,a}$
500_10_15	$0.270 \pm 0.003^{A,a}$	$1.704 \pm 0.021^{B,a}$	$0.254 \pm 0.005^{A,a}$	$1.658 \pm 0.067^{B,a}$	$0.500 \pm 0.187^{A,ab}$	$2.740 \pm 0.132^{A,a}$	$0.274 \pm 0.005^{A,a}$	$1.727 \pm 0.026^{B,a}$
500_20_15	$0.274 \pm 0.006^{B,a}$	$1.713 \pm 0.031^{B,a}$	$0.250 \pm 0.001^{B,a}$	$1.628 \pm 0.026^{B,a}$	$0.515 \pm 0.064^{A,ab}$	$2.777 \pm 0.406^{A,a}$	$0.282 \pm 0.015^{B,a}$	$1.730 \pm 0.006^{B,a}$
500_40_15	$0.279 \pm 0.013^{AB,a}$	$1.722 \pm 0.026^{B,a}$	$0.258 \pm 0.011^{B,a}$	$1.813 \pm 0.134^{B,a}$	$0.466 \pm 0.095^{A,ab}$	$2.367 \pm 0.233^{A,a}$	$0.284 \pm 0.013^{AB,a}$	$1.731 \pm 0.026^{B,a}$

There are some destabilization mechanisms proposed in the literature such as flocculation, coalescence and partial coalescence of droplets (Vanapalli et al., 2002) as explained in the Introduction section. In this study the beginning of slight destabilization on 14th day was mainly attributed to the partial coalescence due to the dispersed oil phase fraction, emulsifier type and ratio characteristics of the prepared emulsions. In addition, the size increase in small size droplets was not abrupt enough to propose an alternative mechanism. The dispersed phase fraction was 10% (w/w) in our study and it was evaluated as a low fraction compared to other emulsion systems containing low to medium and high dispersed volume fractions (φ), $\varphi < 0.5$ and $\varphi \sim 0.5–0.7$, respectively. The emulsifier concentration is ~2% (w/w) and this is also not a very high emulsifier content for oil in water emulsions since some emulsions might contain higher emulsifier concentrations (~ 6% (w/w)) and under these circumstances our emulsion is a dilute sodium caseinate (SC) stabilized emulsion (Dickinson and Golding, 1997). As the storage time increased, previously formed β crystals began to penetrate through the droplet surface and overcome the surface resistance. These needle like crystals then took part in the partial coalescence leading to an increase in droplet size since these surface migrated crystals changed the surfactant conformation on the droplet surface (Sugimoto et al., 2001). Another factor contributing to destabilization is the change in the distribution of emulsifier (SC) between the dispersed and the continuous phase during storage. This originates from the changes in the conformation of SC due to the initial heat treatment. Our emulsified emulsions were initially heated up to 70 °C and this clearly promoted slight changes in the SC conformation (Coupland, 2002). Therefore, during cooling, SC on the droplet surface evoked adsorption of the dissolved SC from the bulk phase on to the droplet surface and this increased the SC concentration at the surface promoting further droplet flocculation and eventually partial coalescence of droplets (Sugimoto et al., 2001). The decline in the bigger droplet size on 28th day with respect to 14th day (Table 3), originated from the diffusion of crystals from one droplet to another. The disruption of oil droplet surfaces by crystal migration from the interiors of the droplet to the surface occurred and this phenomenon altered the droplet shape. Consequently, bigger droplets were disrupted on the 28th day and formation of more disordered α crystals proved this claim.

The oil droplet aggregation which is reported to have a viscosity increasing effect in emulsions is also consistent with the decreasing trend of T_2 at the end of the storage period in our study (Sugimoto et al., 2001). The increased surfactant concentration and merging of droplets probably created new interaction sites for water and droplet surfaces resulting in lower T_2 on the 28th day. The lower SDC similar to T_2 through the end of the storage, proved the more heterogeneous order of droplet size and distribution within the emulsion system. At that point water molecules encountered more impairment and hurdles during diffusing. Moreover, slight increase in α content on 28th day provided more interaction sites for water molecules to interact with droplet surfaces since disordered α lipid crystals had more mobility and interaction sites. These phenomena also contributed to the decrease in T_2 and SDC values.

4. Conclusions

Lipid crystallization behavior of oil in water emulsions containing PS as the dispersed phase and SC as the emulsifier under HHP was studied by DSC and NMR relaxometry. The investigation of DSC curves and relative areas of these curves provided α and β contents. HHP induced formation of more stable β lipid crystals. Changes in α and β contents with respect to pressure and storage time were detected by T_2 and SDC measurements. An increasing trend for T_2 was observed with respect to increase in both pressure and storage time. Formation of β crystals was discernible with the increase in T_2. SDC showed a decreasing trend with increasing pressure but an increasing trend with the storage time. Both T_2 and SDC experienced a decrease on the 28th day of the storage where also a slight increase in α and decrease in β contents were detected for almost all samples. These findings suggested that the beginning of destabilization of emulsions can be detected by NMR measurements. Since HHP provided stable emulsions even for long storage times, aforementioned destabilization of emulsions could not be visually observed. Therefore, this beginning of slight destabilization was justified by NMR measurements in addition to polymorphic changes of lipid crystals. This study demonstrated that HHP produced stable lipid crystal forms, presence and type of emulsifier affected the crystal structures and NMR relaxometry could be recommended as an alternative method to track the polymorphic changes of lipid crystals under pressure treatment and storage.

Funding

This study was supported by Middle East Technical University [grant number BAP-03-14-2016-003].

Conflict of interest

The authors declare that they have no conflict of interest.

Compliance with ethics requirements

This article does not contain any studies with human or animal subjects.

Acknowledgements

We thank Cargill-Turkey and Lipoid AG (Germany) for providing raw materials and chemicals. We would also like to thank Prof. Dr. Behiç Mert (Middle East Technical University) for his help on emulsion preparation and Dr. Leonid Grunin from Volga University of Technology (Mary El, Yoshkar-Ola, Russian Federation) for providing support on self-diffusion measurements.

Appendix A. Supplementary data

Supplementary data related to this article can be found at https://doi.org/10.1016/j.jfoodeng.2017.10.007.

References

Barrabino, A., Keleşoğlu, S., Sørland, G.H., Simon, S., Sjöblom, J., 2014. Phase inversion in emulsions studied by low field NMR. Colloids Surf. A Physicochem. Eng. Asp. 443, 368–376. https://doi.org/10.1016/j.colsurfa.2013.11.016.

Blümer, C., Mäder, K., 2005. Isostatic ultra-high-pressure effects on supercooled melts in colloidal triglyceride dispersions. Pharm. Res. 22, 1708–1715. https://doi.org/10.1007/s11095-005-6949-x.

Boode, K., Walstra, P., 1993. Kinetics of partial coalescence in oil-in-water emulsions. In: Dickinson, E., Walstra, P. (Eds.), Food Colloids and Polymers: Stability and Mechanical Properties. The Royal Society of Chemistry, Cambridge, pp. 23–31.

Bouteille, R., Perez, J., Khifer, F., Jouan-Rimbaud-Bouveresse, D., Lecanu, B., This, H., 2013. Influence of the colloidal structure of dairy gels on milk fat fusion behavior: quantification of the liquid fat content by in situ quantitative proton nuclear magnetic resonance spectroscopy (isq 1H NMR). J. Food Sci. 78, 535–541. https://doi.org/10.1111/1750-3841.12072.

Coupland, J.N., 2002. Crystallization in emulsions. Curr. Opin. Colloid Interface Sci. 7, 445–450. https://doi.org/10.1016/S1359-0294(02)00080-8.

Dickinson, E., Golding, M., 1997. Rheology of sodium caseinate stabilized oil-in-water emulsions. J. Colloid Interface Sci. 191, 166–176.

Dickinson, E., McClements, D.J., 1995. Advances in Food Colloids. Chapman & Hall, London.

Ferstl, P., Eder, C., Ruß, W., Wierschem, A., 2011. Pressure-induced crystallization of

triacylglycerides. High. Press. Res. 31, 339–349. https://doi.org/10.1080/08957959.2011.582870.
Greiff, K., Fuentes, A., Aursand, I.G., Erikson, U., Masot, R., Alcańiz, M., Barat, J.M., 2014. Innovative nondestructive measurements of water activity and the content of salts in low-salt hake minces. J. Agric. Food Chem. 62, 2496–2505. https://doi.org/10.1021/jf405527t.
Mazzanti, G., Mudge, E.M., Anom, E.Y., 2008. In situ rheo-NMR measurements of solid fat content. J. Am. Oil Chem. Soc. 85, 405–412. https://doi.org/10.1007/s11746-008-1227-9.
McClements, D.J., 2005. Food Emulsions Principles, Practices, and Techniques. Food Emulsions Principles, Practices, and Techniques. https://doi.org/10.1093/acprof:oso/9780195383607.003.0002.
Nadakatti, S.M., 1999. Modified data handling for rapid low-field nuclear magnetic resonance characterization of lyotropic liquid crystal composites. J. Surfactants Deterg. 2, 515–521. https://doi.org/10.1007/s11743-999-0100-9.
Oh, J.H., Swanson, B.G., 2006. Polymorphic transitions of cocoa butter affected by high hydrostatic pressure and sucrose polyesters. J. Am. Oil Chem. Soc. 83, 1007–1014. https://doi.org/10.1007/s11746-006-5155-2.
Palanuwech, J., Coupland, J.N., 2003. Effect of surfactant type on the stability of oil-in-water emulsions to dispersed phase crystallization. Colloids Surf. A Physicochem. Eng. Asp. 223, 251–262. https://doi.org/10.1016/S0927-7757(03)00169-9.
Ritzoulis, C., 2013. Introduction to the Physical Chemistry of Foods. Taylor & Francis, Boca Raton.
Rostocki, A.J., Tarakowski, R., Kiełczyński, P., Szalewski, M., Balcerzak, A., Ptasznik, S., 2013. The ultrasonic investigation of phase transition in olive oil up to 0.7 GPa. J. Am. Oil Chem. Soc. 90, 813–818. https://doi.org/10.1007/s11746-013-2223-2.
Salami, S., Rondeau-Mouro, C., van Duynhoven, J., Mariette, F., 2013. PFG-NMR self-diffusion in casein dispersions: effects of probe size and protein aggregate size. Food Hydrocoll. 31, 248–255. https://doi.org/10.1016/j.foodhyd.2012.10.020.
Sevdin, S., Yücel, U., Alpas, H., 2017. Effect of high hydrostatic pressure (HHP) on crystal structure of palm stearin emulsions. Innov. Food Sci. Emerg. Technol. 42, 42–48. https://doi.org/10.1016/j.ifset.2017.05.005.
Sonoda, T., Takata, Y., Ueno, S., Sato, K., 2004. DSC and synchrotron-radiation X-ray diffraction studies on crystallization and polymorphic behavior of palm stearin in bulk and oil-in-water emulsion states. J. Am. Oil Chem. Soc. 81, 365–373. https://doi.org/10.1007/s11746-004-0908-5.
Sugimoto, T., Mori, T., Mano, J.I., Mutoh, T.-A., Shiinoki, Y., Matsumura, Y., 2001. Effects of fat crystallization on the behavior of proteins and lipids at oil droplet surfaces. J. Am. Oil Chem. Soc. 78, 183–188. https://doi.org/10.1007/s11746-001-0241-z.
Tadros, T.F., 2013. Emulsion formation, stability, and rheology. In: Tadros, F.T. (Ed.), Emulsion Formation and Stability. Wiley-VCH Verlag GmbH & Co. KGaA, Weinheim, pp. 1–75.
Van Duynhoven, J., Dubourg, I., Goudappel, G.J., Roijers, E., 2002. Determination of MG and TG phase composition by time-domain NMR. J. Am. Oil Chem. Soc. 79, 383–388. https://doi.org/10.1007/s11746-002-0493-7.
Vanapalli, S.A., Palanuwech, J., Coupland, J.N., 2002. Stability of emulsions to dispersed phase crystallization: effect of oil type, dispersed phase volume fraction, and cooling rate. Colloids Surf. A Physicochem. Eng. Asp. 204, 227–237.
Whittinghill, J., Norton, J., Proctor, A., 2000. Stability determination of soy lecithin-based emulsions by Fourier transform infrared spectroscopy. J. Am. Oil Chem. Soc. 77, 37–42. https://doi.org/10.1007/s11746-000-0006-8.
Yucel, U., Elias, R.J., Coupland, J.N., 2013. Localization and reactivity of a hydrophobic solute in lecithin and caseinate stabilized solid lipid nanoparticles and nanoemulsions. J. Colloid Interface Sci. 394, 20–25. https://doi.org/10.1016/j.jcis.2012.12.042.
Zhang, R., Huo, J., Peng, Z., Feng, Q., Wang, J., Zhang, J., 2016. Research on oil-based drilling fluids emulsion droplet by low-field NMR. Appl. Magn. Reson 47, 1339–1352. https://doi.org/10.1007/s00723-016-0845-x.
Zulkurnain, M., Maleky, F., Balasubramaniam, V.M., 2016a. High pressure crystallization of binary fat blend: a feasibility study. Innov. Food Sci. Emerg. Technol. 38, 302–311. https://doi.org/10.1016/j.ifset.2016.06.025.
Zulkurnain, M., Maleky, F., Balasubramaniam, V.M., 2016b. High pressure processing effects on lipids thermophysical properties and crystallization kinetics. Food Eng. Rev. 8, 1–21. https://doi.org/10.1007/s12393-016-9144-4.